SIMULATION OF SEMICONDUCTOR DEVICES AND PROCESSES Vol. 3
Edited by G. Baccarani, M. Rudan - Bologna (Italy) September 26-28, 1988 - Tecnoprint

2D AND 3D CAPACITANCE CALCULATIONS FOR VLSI STRUCTURES USING THE ENERGY METHOD

W.-E. Matzke*, K. Gärtner**, B. Heinemann*

*Institute for Physics of Semiconductors of the Academy of Sciences of the GDR, Frankfurt(O), GDR

**Karl-Weierstraß-Institute of Mathematics of the Academy of Sciences of the GDR, Berlin, GDR

SUMMARY

A numerical method based on a domain integral representation of the charge for the determination of the capacitance coefficients of VLSI structures is given. This method is refered to as energy method. It is shown how this method can be extended to situations where the simulation area contains semiconductor regions. In order to verify the formulation and numerical accuracy, the reader is provided with two fully described standard sample problems. Furthermore, a 4 Mb DRAM cell as an example of a very complex 3D wiring structure including semiconductor regions is considered.

INTRODUCTION

The necessity to calculate accurately the capacitances of interconnection wires of today's multilevel VLSI circuits is indisputable in order to ensure a succesful chip design (Fichtner, 1983). Besides integral equation methods, domain methods are used frequently for capacitance calculation. Using domain methods, the problem of capacitance evaluation is attributed to charge evaluation. Recently, as alternative to the usually used boundary integral representation of the charge, Straker (1986), Klose (1987) and Matzke (1988a) have discussed a charge calculation method based on a domain inte-

gral formulation of the charge (energy method). This method enhances the accuracy of the results. For detailed insight into the domain integral formulation of the charge in connection with domain methods, see Matzke (1988b). However, up to now this method was limited to situations where the simulation area contains no semiconductor regions. Hence, it is the main purpose of this paper to give an extension of the energy method to these cases.

REMARKS ON THE PROBLEM

Let us consider a system of N conductors (interconnection wires) and some reference conductor. The N conductors may be surrounded by dielectric media and semiconductor materials. Often there does not exist pronounced influence of the semiconductor regions on the capacitances to be determined. Hence it is possible to neglect the semiconductor regions (linear case). In other situations for the accurate prediction of the capacitances it is necessary to take into account the semiconductor regions. The non-linearity appearing in these cases arises from the non-linear potential dependent charge carrier density of the semiconductor materials (non-linear case). Since this paper is concerned exclusively with reverse biased junctions (junction capacitances), in so far as we consider capacitances between semiconductor regions, it is possible to assume the electron and hole current densities in the semiconductor regions to be exactly zero (zero-current case (Polak, 1987)). Furthermore, we neglect the minority carriers. Boltzmann's statistic is used to model the density of majority carriers. The quasi-Fermi potential for majority carriers is set to the known constant terminal potential applied to the conductor which contacts the corresponding semiconductor region.

We assume that the reference conductor as well as the remaining N conductors are biased with prescribed potentials. Without loss of generality the reference conductor potential is assumed to be constant. A given set of such potentials is called bias point. Let $\delta Q=(\delta Q_1,..,\delta Q_N)^T$ be the vector of changes of total charges on the N conductors due to conductor potential perturbations $\delta\psi=(\delta\psi_1,..,\delta\psi_N)^T$. The relationship between the changes of total char-

ges on the N conductors and the corresponding conductor potential perturbations is given by

$$\delta Q = C_S \delta \psi \tag{1}$$

where C_S is the NxN short-circuit capacitance matrix. The elements of C_S are

$$C_{Sij} = \delta Q_i^{(j)} / \delta \psi_j \tag{2}$$

where $\delta Q_i^{(j)}$ is the change of charge on conductor i due to a potential perturbation $\delta \psi_j$ on conductor j when the potentials of all other conductors remain unperturbed. The two terminal capacitances C_{io}, C_{ij} and C_{ii} as usually used by the circuit designer are obtained from the short-circuit capacitances by the well known relationships (e.g. Ruehli, 1975)[1].

In our paper we calculate the capacitances directly from the above definition. A prerequisite for the direct use of equation (2) is the existence of conductors with non-vanishing surface charge densities. However, as it is well known, at a contact (conductor/semiconductor interface) the space charge density is assumed to be zero. Therefore, there is no surface charge on the conductor at the contact. There are different methods to overcome this difficulty. One is to assume the existence of an equipotential surface along the pn-junction (Straker, 1984). Another is to extent this assumption by replacing heavily doped semiconductor regions by conductors. The latter offers the possibility of simple applicability of the energy method.

THE ENERGY METHOD

With reference to Fig.1, let Ω be the bounded Lipschitzian domain under consideration. The boundary Γ of the domain Ω is the union of the outer boundary Γ_o and the internal boundaries Γ_i (i=1,.., N). The latter are given by the conductor surfaces. Γ_o can be split in into two classes ($\Gamma_o = \Gamma_{oD} \cup \Gamma_{oN}$). Γ_{oD} denotes parts of Γ_o corresponding to boundary

[1] C_{io} is the capacitance between conductor i and the reference conductor, C_{ij} is the coupling capacitance between conductor i and j and C_{ii} denotes the total capacitance of conductor i.

conditions of the Dirichlet type. Usually, Γ_{oD} is given by the reference conductor. Γ_{oN} represents parts of Γ_o with boundary conditions of the Neumann type. Γ_{oN} is in principle an artificial boundary which has to be introduced to obtain a bounded domain and to consider symmetries. Note, that Γ_{oD} may also contain parts of the artificial boundary, because it is sometimes more convenient to introduce Dirichlet boundary conditions. Furthermore, let n be the outward unit normal at Γ and γ_i a test function ($\gamma_i \in W^{1,2}(\Omega)$ where $W^{1,2}$ denotes the appropriate Sobolov space) satisfying the following boundary conditions:

$$(3) \qquad \gamma_i = \begin{cases} 1 \text{ on } \Gamma_i \\ 0 \text{ on } \Gamma \setminus \Gamma_i \setminus \Gamma_{oN} \end{cases} \quad \text{and} \quad \frac{\partial \gamma_i}{\partial n} = 0 \text{ on } \Gamma_{oN}.$$

The change of stored charge $\delta Q_i^{(j)}$ on conductor i due to a potential perturbation $\delta\psi_j$ on conductor j follows from Gauss`s law as

$$(4) \qquad \delta Q_i^{(j)} = \int_{\Gamma_i} \varepsilon \nabla \delta\psi^{(j)} \cdot n \, ds$$

where ε is the electric permittivity and $\delta\psi^{(j)}$ is the perturbation of the potential distribution ψ of the considered bias point. The resulting potential distribution $\psi + \delta\psi^{(j)}$ is the weak solution (ψ, $\delta\psi^{(j)} \in W^{1,2}(\Omega)$) satisfying the following boundary value problem:

$$(5a) \qquad -\nabla \cdot \varepsilon \nabla (\psi + \delta\psi^{(j)}) = \varrho(\psi + \delta\psi^{(j)}) \text{ in } \Omega$$

$$\psi + \delta\psi^{(j)} = \psi_j + \delta\psi_j \text{ on } \Gamma_j$$

$$(5b) \qquad \psi + \delta\psi^{(j)} = \psi_i \text{ on } \Gamma_i \;,\; i \neq j = 1, \ldots . N$$

$$\psi + \delta\psi^{(j)} = \psi_o \text{ on } \Gamma_o \;,\; \frac{\partial}{\partial n}(\psi + \delta\psi^{(j)}) = 0 \text{ on } \Gamma_{oN}$$

where ϱ is the space charge density. In semiconductor regions the space charge density is given by $\varrho = q(m+D)$ where q is the elementary charge and D represents the doping (fixed charges). m denotes the majority carrier concentration (electrons or holes):

$$(6) \qquad m = \begin{cases} n_i \exp((\varphi - \psi)/V_T), & \text{p-type semicond.} \\ -n_i \exp((\psi - \varphi)/V_T), & \text{n-type semicond.} \end{cases}$$

where n_i is the intrinsic concentration, V_T is the thermal voltage and φ denotes the quasi-Fermi potential of majority carriers.

In principle (existence supposed) it is possible to calculate the desired changes of charges directly from relationship (4) by evaluating a boundary integral. However, in our paper, we will take a different approach, based on a variational formulation. For all test functions γ_i (fulfiling boundary condition (3)) the integral in equation (4) may be rewritten as a boundary integral where the integration is performed over the whole boundary Γ. By using Green's first identity it is possible to transform this boundary integral into domain integrals:

$$\delta Q_i^{(j)} = \int_\Omega \gamma_i \nabla \cdot \varepsilon \nabla \delta\psi^{(j)} dv + \int_\Omega \varepsilon \nabla \delta\psi^{(j)} \nabla \gamma_i dv. \tag{7}$$

With respect to relationship (1) an expansion of ϱ in a series at the potential distribution ψ of the considered bias point for sufficiently small $\delta\psi^{(j)}$ yields $\varrho(\psi+\delta\psi^{(j)}) = \varrho(\psi)+(\partial\varrho/\partial\psi)\,\delta\psi^{(j)}$ and hence we have from equation (5a)

$$(-\nabla\cdot\varepsilon\nabla - \frac{\partial\varrho}{\partial\psi})\,\delta\psi^{(j)} = 0\ ,\ -\frac{\partial\varrho}{\partial\psi} = -q\frac{\partial m}{\partial\psi} \geqslant 0. \tag{8}$$

Thus equation (7) may be written as

$$\delta Q_i^{(j)} = \int_\Omega \varepsilon \nabla \delta\psi^{(j)} \nabla \gamma_i \, dv - \int_\Omega \frac{\partial\varrho}{\partial\psi} \delta\psi^{(j)} \gamma_i \, dv \tag{9}$$

for all test functions γ_i[2]. However, $\gamma_i = \delta\psi^{(i)}/\delta\psi_i$ is an admissible test function and finally we have

$$\delta Q_i^{(j)} = \delta\psi_i^{-1} \left(\int_\Omega \varepsilon \nabla \delta\psi^{(i)} \nabla \delta\psi^{(j)} dv - \int_\Omega \frac{\partial\varrho}{\partial\psi} \delta\psi^{(i)} \delta\psi^{(j)} dv \right). \tag{10}$$

Note, the right hand side of equation (10) is proportional to the second-order change in energy of stored charge associated with conductor i. In particular, the first domain integral is related to second-order changes in total energy of the electrostatic field whereas the second domain integral is related to second-order changes in energy of the

[2]Remark: The freedom in the choice of the test function γ_i can be used to compute all capacitances associated with conductor j -that is, column j or line j respectively, of Cs- with only one solution of the boundary value problem (5).

space charge. In the linear case the second domain integral in relationship (10) vanishes and the first one has the following physical meaning. For i=j it represents double the self-energy of the total charge on conductor j when all conductors except conductor j are grounded. For i≠j it corresponds to the interaction energy between the total charge on conductor i and the total charge on conductor j when all conductors except conductor i and j are grounded.

For i=j, equation (8) is the Euler-Lagrange equation of the positive quadratic functional $\delta Q_j^{(j)}$ given by relationship (10), this means $\delta Q_j^{(j)}$ is minimized by the solution $\delta\psi^{(j)}$. With the boundary conditions (5b) equation (8) has an unique solution $\delta\psi^{(j)}(x)>0$ for $x\in\Omega$ and from maximum principle follows: (i) A local minimum $\delta\psi^{(j)}(x_0)$, $x_0\in\Omega$ is possible, but only with $\delta\psi^{(j)}(x_0)>0$. (ii) A local maximum does not exist for $x_0\in\Omega$. Thus we have $n_j\cdot\nabla\delta\psi^{(j)}>0$ on Γ_j and $n_i\cdot\nabla\delta\psi^{(j)}<0$ on Γ_i ($i\neq j=1,..,N$), that is $Cs_{jj}>0$ and $Cs_{ij}=Cs_{ji}<0$, the classical properties of Cs.

The given properties can be carried over to the discret problem and for different discret problems $(\delta\psi^{(j)})^k\in V^k$ and $(\delta\psi^{(j)})^{k+1}\in V^{k+1}$ with $V^k\subset V^{k+1}$ where V^k and V^{k+1} denoting appropriate vectorspaces we have (with "frozen" n_i,ψ) $Cs_{jj}((\delta\psi^{(j)})^k)\geq Cs_{jj}((\delta\psi^{(j)})^{k+1})$ because the functional $\delta Q_j^{(j)}$ and therefore Cs_{jj} can not increase for a larger space. Thus an upper bound for the total capacitances has been obtained.

NUMERICAL RESULTS

The following section presents numerical results of three sample problems. The first two examples (a three conductor problem and two crossing conductors above a ground plane) are taken from Quint (1987). The last example (4 Mb DRAM cell Murkin (1987)) was chosen to show the complexity of a real problem.

Fig.2 illustrates the two-dimensional three conductor problem. We applied several programs (capable of solving Poisson's equation together with the respective boundary conditions) to solve this problem. TOSCA (Gajewski, 1986) is a 2D device simulator which is based on the finite-element method (FEM). By 3_D_pgm we denote a 3D program

which is actual under development by one of the authors. This program uses a finite difference discretization scheme (FDM). Equation (10) is the basis of all numerical results obtained via these two programs. BEM denotes a boundary element method program (Streese, 1988).

The total capacitance per unit length C_{22} versus the separation S is shown in Fig.3. Fig.4 shows the coupling capacitance per unit length C_{12} versus S. Finally, Fig.5 illustrates the dependence of the coupling capacitance per unit length C_{13} on S. Corresponding to the used different program packages and/or boundary conditions applied on the artificial boundary, in each of these figures five curves are shown. In the case of the curves `3_D_pgm`, `BEM,du/dn=0` and `TOSCA` respectively, we have used an artificial boundary with a homogeneous Neumann boundary condition, which as natural boundary condition minimizes C_{Sij} for fixed Ω, too. The curve `TOSCA,u=0` corresponds to the case of an artificial boundary with a boundary condition of the Dirichlet type ($\psi_o=0$ on Γ_{oD}, $\Gamma_o=\Gamma_{oD}$). With the help of the boundary element method it is possible to solve correctly the real physical situation of the half space. The data obtained for this case (curve `BEM half sp`) should be the basis for the discussion of both the results obtained from the other program packages and the usefulness of the different simple boundary conditions, which are possible for the artificial boundary. The total capacitance per unit length C_{22} of the central conductor increases with decreasing separation S, as shown in Fig.3. The systematic differences between the results obtained by TOSCA and the other programs result from a lower number of grid points (974 points). The results correspond well to the data obtained via 3_D_pgm for a grid with 49x22 points (see table 1). It should be noted that the results for Neumann boundary conditions on the artificial boundary are closer to half space solution than the data obtained for a artificial boundary with Dirichlet boundary condition. Fig.3 contains additional a sixth curve which is obtained from the empirical formula given by Sakurai (1983). Corresponding to expectations the coupling capacitances per unit length C_{12} and C_{13} increase with decreasing separation S (Fig.4 and Fig.5 respectively). As can be seen by reference to Fig.5, a Neumann boundary condition on the artificial bound-

ary yields to a larger coupling capacitance C_{13} in comparision with a Dirichlet boundary condition. Tables 1, 2 and 3 present the numerical data calculated by 3_D_pgm. Table 2 is devoted to the problem "What happens to the unexperienced user ?" and is typical for situations found in 3D problems with complex geometrical structure and limited numbers of grid points, too. Note that the calculated values of the total capacitances decrease with increasing degree of grid refinement. Fig.6 illustrates the potential distribution for the case when both the left as well as the right conductor are grounded whereas the central conductor is set to $\psi_2 > 0$. Partial energy density distributions belonging to this case are shown in Fig.7. For clearness we have only depicted the portion of the total energy density originated in the vertical derivative of the potential. In this sense, Fig.7a illustrates a partial self-energy density distribution whereas Fig.7b shows the distribution of the partial interaction energy density. From these figures an impression of the singularities of $\nabla\psi$ at the conductor corners can be obtained.

The next example considered, is the problem of two crossing conductors above a ground plane. Due to symmetry only a quarter of the original configuration has to be considered, as illustrated in Fig.8. Fig.9 shows total and coupling capacitances of this configuration for two different degrees of grid refinement versus the distance d between the crossing conductors. The capacitance values are obtained via 3_D_pgm. The grid refinement yields a decrease of calculated capacitance values. The total capacitances C_{11} and C_{22} as well as the coupling capacitance C_{12} decrease with increasing distance d. Table 4 presents the capacitance matrices for different distances d (d=0.2,0.4,1.0,2.0 µm).

The last problem considered is a 4 Mb DRAM cell. We have considered a structure consisting of two half cells, as illustrated in Fig.10 where the following abbreviations are used: bli *bit-line i*, wli *word-line i*, hli *main word-line i* (i=1,2),pl *plate* and semi_c *semiconductor*. The voltage dependence of the bit-line 1 capacitance for a half cell (Cbl1) is shown in Fig.11, curve `C` (Cbl1=1.46 fF at 1V; 41x25x61 points and Cbl1=1.40 fF at 1V; 81x49x121 points). Curve `(grad u)**2` represents

double the second-order term of change in total electrostatic energy whereas curve `(-u, d rho)` is proportional to the second order term of change in energy of the space charge. The data obtained for a refined grid are also shown in Fig.11 for a bit-line potential of 1V.

ACKNOWLEDGMENT

The authors wish to thank their colleagues for helpful discussions and especially Dr. H. Streese providing the authors with the numerical results obtained via the boundary element method.

REFERENCES

Fichtner W. and others (1983). Semiconductor Device Simulation. *IEEE Trans. Electron Devices, 30,* 1018-1030.

Gajewski H. and others (1986). *TOSCA User's Guide.* Karl-Weierstraß-Institut für Mathematik der Akademie der Wissenschaften der DDR, Berlin.

Klose H. and others (1987). CAPCAL - 3D Capacitance calculation for application in integrated circuits. *Proc. Symp. on ULSI Science & Technology,* Philadelphia, pp. 671-681.

Matzke W.-E. and others (1988a). 2D-Simulation der parasitären Kapazitäten paralleler Verbindungsleitungen in integrierten MOS-Schaltkreisen unter Berücksichtigung des Programmsystems TOSCA. *Nachrichtentechnik Elektronik, 38,* 27-33.

Matzke W.-E. and others (1988b). On the Calculation of the Capacitance Coefficients for VLSI Multilevel Metallization Lines by Using Domain Methods. *to be published.*

Murkin P.A. and others (1987). Isolation-Related Leakage in a 4 Mb DRAM Cell. *Proc. ESSDERC 87,* Bologna, pp. 761-764.

Polak S.J. and others (1987). Semiconductor Device Modeling from the Numerical Point of View. *Int. J. Num. Methods Eng.*, 24, 763-838.

Quint J.H.M.M. and others (1987). 2-D and 3-D Capacitance Effects in MOS VLSI. *Proc. ESSDERC 87,* Bologna, pp. 417-420.

Ruehli A.E. and Brennan P. (1975). Capacitance Models for Integrated Circuit Metallization Wires.

Table 1. Capacitance matrices for different grids, 3_D_pgm, fF/1.0e-6m, S = 1.5e-6m

points_x
x points_y
49 x 22

	1	2	3
1	0.187	-0.0348	-0.00495
2	-0.0348	0.196	-0.0348
3	-0.00495	-0.0348	0.187

97 x 43

1	0.184	-0.0341	-0.00484
2	-0.0341	0.193	-0.0341
3	-0.00484	-0.0341	0.184

193 x 85

1	0.183	-0.0338	-0.00481
2	-0.0338	0.192	-0.0338
3	-0.00481	-0.0338	0.183

Table 2. Capacitance matrices for simple grids, 3_d_pgm, fF/1.0e-6m, S = 1.5e-6m

points_x
x points_y
10 x 6

	1	2	3
1	0.258	-0.0560	-0.00595
2	-0.0560	0.265	-0.0560
3	-0.00595	-0.0560	0.258

19 x 11

1	0.210	-0.0405	-0.00523
2	-0.0405	0.218	-0.0405
3	-0.00523	-0.0405	0.210

37 x 21

1	0.193	-0.0361	-0.00496
2	-0.0361	0.202	-0.0361
3	-0.00496	-0.0361	0.193

Table 3. Boundary element method (40 linear nonaequidist. elements per conductor), half space

S = 1.0e-6m, fF/1.0e-6m

	1	2	3
1	0.19484	-0.051713	-0.002719
2	-0.051653	0.21656	-0.051653
3	see 1		

S = 1.5e-6m, fF/1.0e-6m

1	0.18223	-0.031919	-0.002508
2	-0.031820	0.19126	-0.031820

S = 2.0e-6m, fF/1.0e-6m

1	0.17745	-0.021844	-0.002265
2	-0.021749	0.18143	-0.021749

Table 4. Two crossing conductors (quarter cell), capacitance matrices for two grids, C / fF, 3_D_pgm

d=0.2e-6m, 30x30x26, 59x59x51 points

	1	2	1	2
1	0.827	-0.186	0.805	-0.178
2	-0.186	0.731	-0.178	0.713

d=0.4e-6m, 30x30x26, 59x59x51 points

1	0.787	-0.144	0.766	-0.138
2	-0.144	0.669	-0.138	0.653

d=1.0e-6m, 30x30x28, 59x59x55 points

1	0.753	-0.105	0.734	-0.101
2	-0.105	0.586	-0.101	0.573

d=2.0e-6m, 30x30x30, 59x59x59 points

1	0.736	-0.0811	0.718	-0.0782
2	-0.0811	0.518	-0.0782	0.508

IEEE J. Solid-State Circuits, 10, 530-536.

Sakurai T. and Tamaru K. (1983). Simple Formulas for Two- and Three-dimensional Capacitances. *IEEE Trans. Electron Devices, 30*, 183-185.

Straker F. and Selberherr S. (1984). Capacitance Computation for VLSI Structures. *Proc. SISDEP 84*, Swansea, pp. 39-55.

Straker F. (1986). *VLSICAP User's Guide*. Institut für Allgemeine Elektrotechnik und Elektronik der Technischen Universität Wien, Wien.

Streese H. (1988). *BESSY: Ein System zur Lösung ebener Probleme mit der Randelementmethode*. Report R-MATH-03/88, Karl-Weierstraß-Institut für Mathematik der Akademie der Wissenschaften der DDR, Berlin.

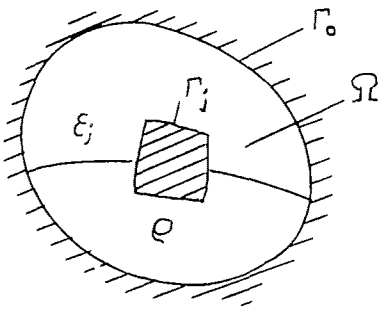

Figure 1

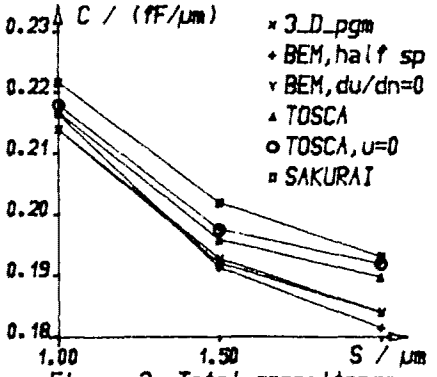

Figure 3: Total capacitance C22

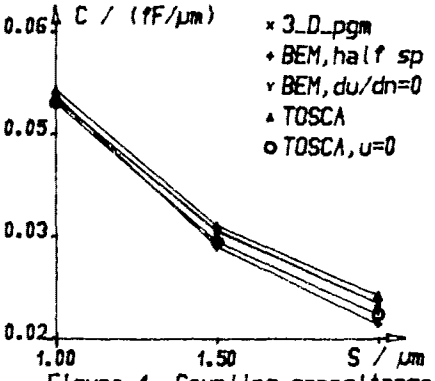

Figure 4: Coupling capacitance C12

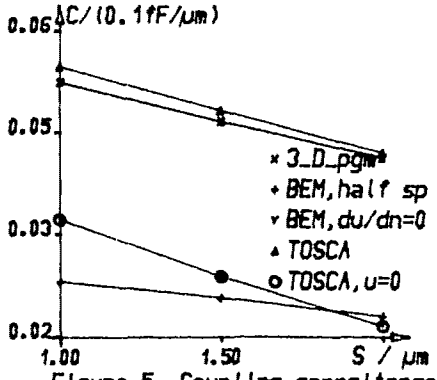

Figure 5: Coupling capacitance C13

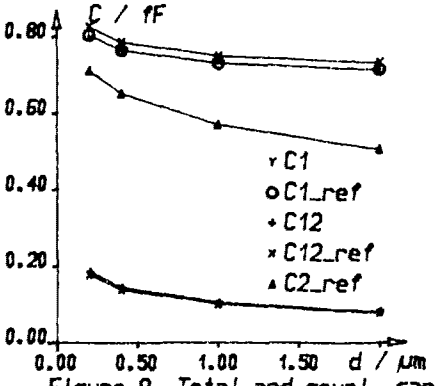

Figure 9: Total and coupl. cap. crossing conduct. (quart. cell)

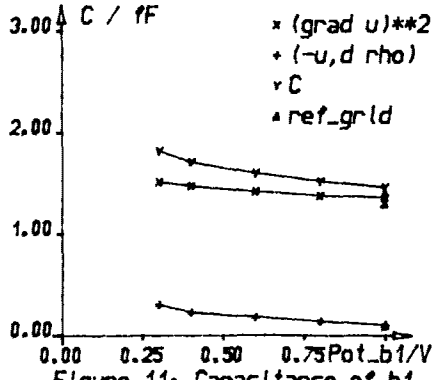

Figure 11: Capacitance of b1, half cell, Pot_b1=0 : th. equ.

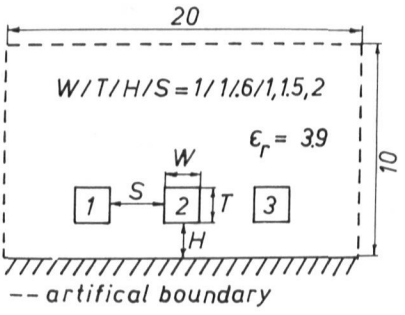

Fig. 2. Three conductor problem

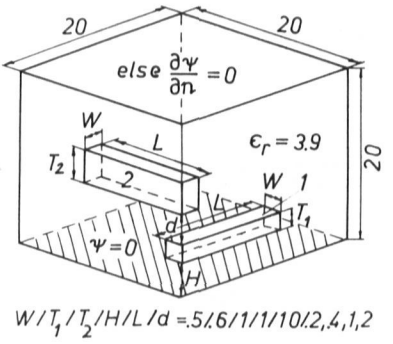

Fig. 8. Crossing conductors

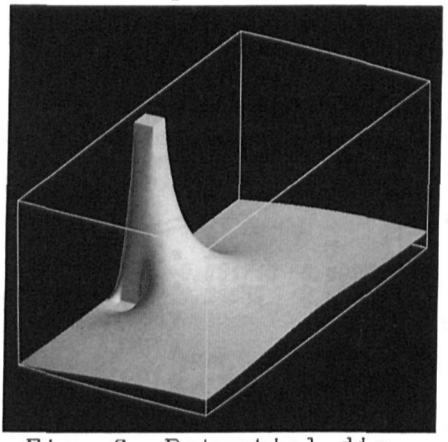

Fig. 6. Potential distribution

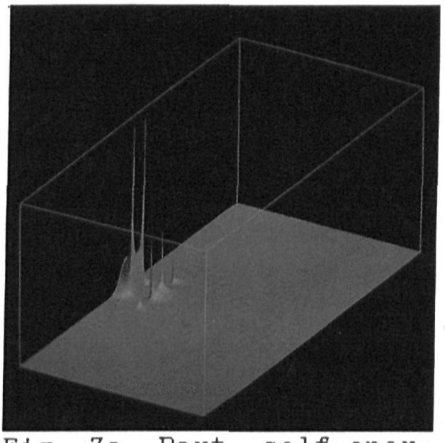

Fig. 7a. Part. self-energy dens. distribution

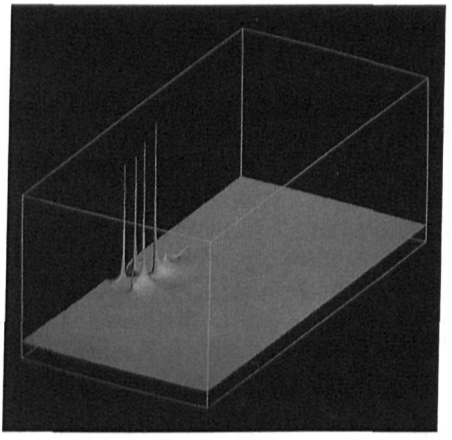

Fig. 7b. Part. interact. energy dens. distribution

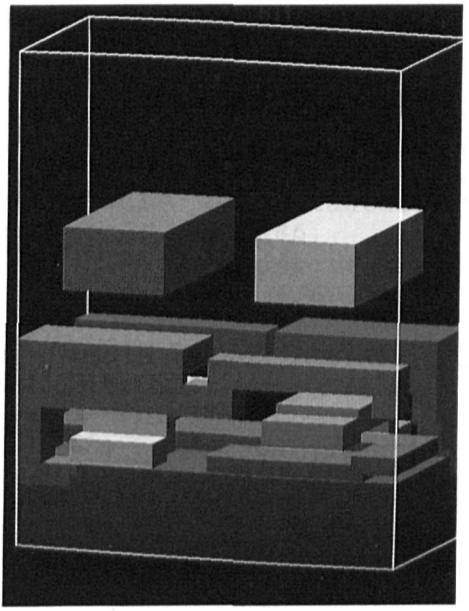

Fig. 10. 4Mb DRAM cell